ACCOUNTING FOR MEMBRANE PROPERTIES IN THE MATHEMATICAL MODELS OF HIGH-PRESSURE MEMBRANE CONTACTORS FOR NATURAL GAS SWEETENING

Ven Chian Quek[1,2], Nilay Shah[1], and Benoît Chachuat[1*]

[1] Centre for Process Systems Engineering, Department of Chemical Engineering, Imperial College London, South Kensington Campus, London SW7 2AZ, UK

[2] Group Research & Technology, PETRONAS, 50088 Kuala Lumpur, Malaysia

Abstract

Membrane contactors (MBC) are a promising technology for natural gas sweetening applications due to their large intensification potential compared with conventional absorption towers. This paper develops a mathematical model for improved understanding of a novel MBC operating at high pressure. This model accounts for the effect of membrane pore-size distribution on membrane (partial) wetting in order to accurately predict CO_2 absorption performance. The membrane wetting and CO_2 absorption performance of two (2) industrial-scale MBC modules with different membrane characteristics are reported as a case study. The effect of key operating conditions, such as the liquid flow rate and the operating temperature is analysed. The effect of operating an MBC module in vertical or horizontal mode is also investigated. The results confirm the need to account for the membrane properties for accurate prediction of the membrane wetting, thereby justifying the proposed model extension.

Keywords

Membrane contactor; Natural gas sweetening; CO_2 absorption; Pore size distribution; Wetting ratio

1. Introduction

A new hybrid process combining the advantages of both conventional chemical absorption and membrane separation, called membrane contactor (MBC), has been gaining significant attention over the past decade. MBC is considered a promising process for intensification purposes as it can provide high specific surface areas, control over the gas and liquid flow rates independently, modularity, and compactness (Lu et al. 2008). Recent research has shown that MBC may offer significant benefits by virtue of a smaller physical footprint and by eliminating operational challenges such as flooding, channelling, foaming and liquid entrainment faced by conventional absorption towers (Boributh et al. 2011).

In natural gas sweetening applications, MBC provides a means of removing CO_2, without the gas and liquid phases mixing into each other, as illustrated in Figure 1. The gas phase is separated from the liquid phase by a microporous hollow fibre membrane (HFM), and a highly selective separation may be obtained by using similar solvents as in conventional absorption towers.

The non-wetted model of MBC operation (see Figure 1a) is preferred in practice as it presents a higher CO_2 absorption rate. When partially (Figure 1b) or fully filled (Figure 1c) with liquid , the membrane pores quickly increase the membrane mass transfer resistance, leading to economically unfavourable operation (Mansourizadeh & Ismail 2009). For instance, Wang et al. (2005) argue that a change in the wetting ratio as small as 5% can lead to a 20% reduction in mass transfer rate.

Mathematical models provide an effective tool to better understand the CO_2 removal process in MBC, and therefore

*Corresponding author. Tel.: +44 (0)207 594 5594. E-mail: b.chachuat@imperial.ac.uk

allow a better assessment and optimisation of their performance. Chabanon et al. (2013) have conducted a comparison of different modeling approaches for CO_2 absorption with MBC, from the simplest (constant K) to the more complex 2-D models. This comparison is established on the basis of a single adjustable parameter, namely the membrane mass-transfer coefficient (k_m). It is rather common to treat the wetting ratio as another adjustable parameter in MBC models (Al-Marzouqi et al., 2008; Faiz et al., 2010; Boributh et al., 2011). For instance, Lu et al. (2008) and Cui et al. (2015) have shown that a better agreement with experimental data can be obtained by accounting for such partial wetting.

While several mathematical models describing the degree of membrane wetting and CO_2 absorption mechanism have been developed for low-pressure MBC applications such as post- combustion, very few studies have focused on high-pressure operation, e.g., for natural gas sweetening applications. Recently, Faiz et al. (2010) have studied the physical and chemical absorption of CO_2 in natural gas at the pressure between 10 and 50 bar, finding a good agreement between mathematical models and experiments by considering the wetting ratio as an adjustable parameter.

Through this work, we develop a mathematical model that incorporates both the pore size distribution and the Laplace equation for improved prediction of CO_2 absorption in natural gas sweetening under industrially relevant operating conditions. The developed model can predict the variation in membrane wetting along the fibre length, thereby making it possible to investigate the effect of different membrane characteristics, gas and liquid flow rates, operation temperatures, and module orientation on MBC performance.

The rest of the paper is organised as follows. The mathematical model is presented in Section 2, followed by the numerical case study definition in Section 3, the results and discussions in Section 4, before drawing conclusions in Section 5.

2. MBC Model Development

2.1. Mass-balance equations

The schematic diagram of an MBC in Figure 2 shows four domains: (i) tube; (ii) membrane-dry; (iii) membrane-wet; (iv) shell. The solvent flows inside the shell (at z = 0), and the CO_2 contained in the gas phase flows in the tube (at z=L), here in a counter-current configuration. The shell area between the fibres depends on the actual packing, and it is convenient to approximate the shell cross-section surrounding each fibre with a circle (radius r_3). Then, Harpel's free surface model can be used to describe the velocity profile inside the shell (Mansourizadeh & Ismail 2009). The gas mixture diffuses from the tube through the fibre walls into the shell where only CO_2 absorbs into, and then reacts with, the solvent; CH_4 absorption in the solvent may be neglected due to its very low solubility.

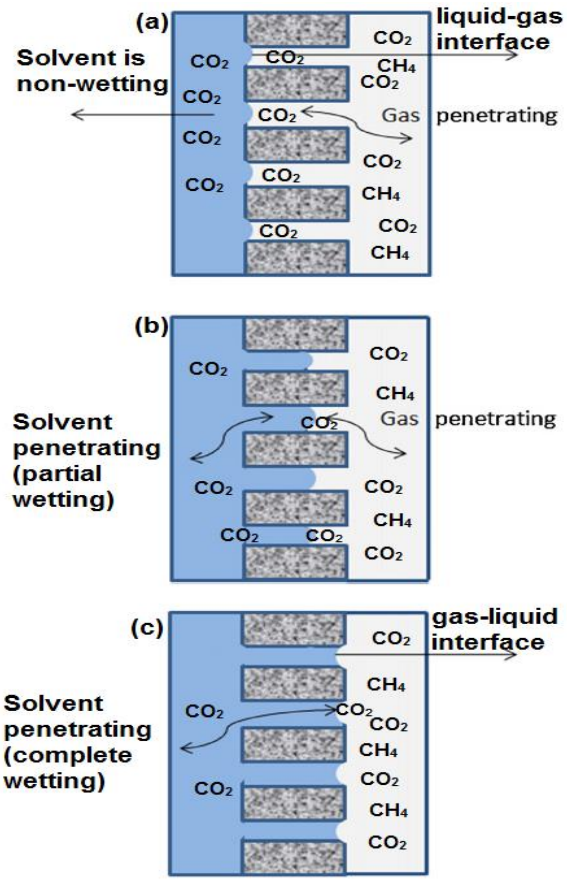

Figure 1. *Principle of MBC and wetting phenomena within the membrane: (a) non wetted; (b) partially-wetted; (c) fully wetted (Faiz et al., 2010).*

The key assumptions used in MBC model are consistent with published models in the literature, and summarised below:

1. Cylindrical geometry;
2. Steady state and isothermal operation;
3. Compressibility factor based on real gas behaviour;
4. Laminar liquid and gas flows with fully developed velocity profiles;
5. Negligible convective mass transfer in pores due to their small size;
6. Gas-liquid equilibrium following Henry's law;
7. Membrane properties both uniform in space and constant over time.

The general equation describing transport of the species $i \in \{CO_2, \mathrm{Sol}\}$ at steady state in a 2-D cylindrical coordinates is given by:

$$v_z \frac{\partial c_i}{\partial z} = D_i \left(\frac{\partial^2 c_i}{\partial r^2} + \frac{1}{r}\frac{\partial c_i}{\partial r} + \frac{\partial^2 c_i}{\partial z^2} \right) + R_i \qquad (1)$$

Specialisations of this conservation equation in the tube, membrane and shell sections, and their associated boundary conditions, are listed in Table 1.Expressions for the reaction rates, the distribution and diffusivity coefficients as well as the module specifications are given in Section 3.

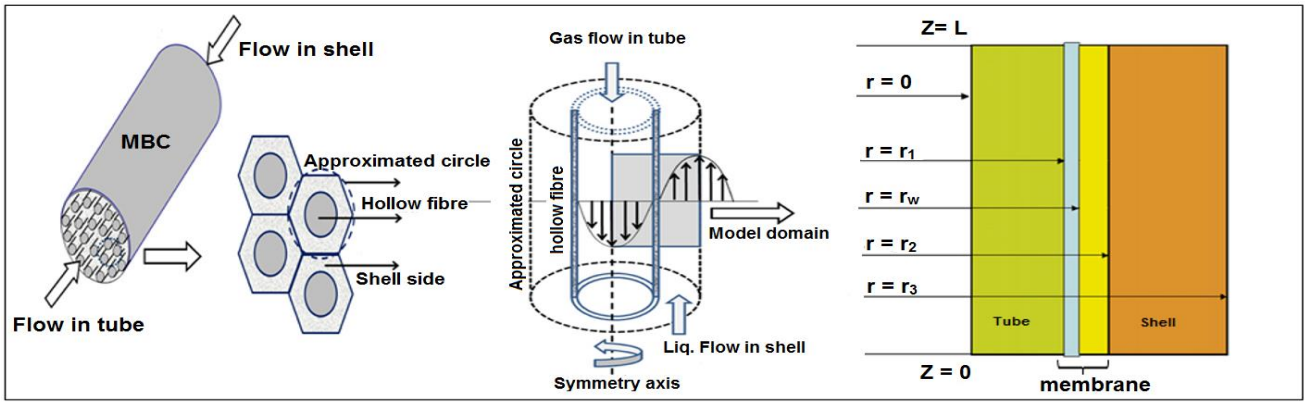

Figure 2. *Schematic diagram of an MBC with four conceptual domains as tube, membrane-dry, membrane-wet and shell.*

Table 1: *Summary of conservation equations and boundary conditions in each domain.*

Section	Material Balances
Tube	$v_{z,g}\frac{\partial C_{CO_2,t}}{\partial z} = D_{CO_2,g}\left[\frac{\partial C_{CO_2,t}}{\partial r^2} + \frac{1}{r}\frac{\partial C_{CO_2,t}}{\partial r} + \frac{\partial^2 C_{CO_2,t}}{\partial z^2}\right]$
Membrane Dry	$D_{CO_2,md}\left[\frac{\partial C_{CO_2,md}}{\partial r^2} + \frac{1}{r}\frac{\partial C_{CO_2,md}}{\partial r}\right] = 0$
Membrane wetted	$D_{i,mw}\left[\frac{\partial C_{i,mw}}{\partial r^2} + \frac{1}{r}\frac{\partial C_{i,mw}}{\partial r}\right] + R_i = 0$
Shell	$v_{z,l}\frac{\partial C_{i,s}}{\partial z} = D_{i,l}\left[\frac{\partial C_{i,s}}{\partial r^2} + \frac{1}{r}\frac{\partial C_{i,s}}{\partial r} + \frac{\partial^2 C_{i,s}}{\partial z^2}\right] + R_i$
	Boundary Conditions
z=0;Tube	$\frac{\partial C_{CO_2,t}}{\partial z} = 0$
z=L; Tube	$C_{CO_2,t} = C_{CO_2}^{in}$
z=0; Shell	$C_{CO_2,s} = 0$ $C_{Sol,s} = C_{Sol}^{in}$
z=L; Shell	$\frac{\partial C_{i,s}}{\partial z} = 0$
r=0	$\frac{\partial C_{CO_2,t}}{\partial r} = 0$
r=r_1	$C_{CO_2,t} = C_{CO_2,md}$ $D_{CO_2,g}\frac{\partial C_{CO_2,t}}{\partial r} = D_{CO_2,md}\frac{\partial C_{CO_2,md}}{\partial r}$
r=r_w	$C_{CO_2,mw} = m\, C_{CO_2,md}$ $\frac{\partial C_{Sol,mw}}{\partial r} = 0$ $D_{CO_2,mw}\frac{\partial C_{CO_2,mw}}{\partial r} = D_{CO_2,md}\frac{\partial C_{CO_2,md}}{\partial r}$
r=r_2	$C_{i,mw} = C_{i,s}$ $D_{i,l}\frac{\partial C_{i,s}}{\partial r} = D_{i,mw}\frac{\partial C_{i,mw}}{\partial r}$
r=r_3	$\frac{\partial C_{i,s}}{\partial r} = 0$

2.2 Modelling of the wetting ratio

For a given hydrophobic material, the degree of membrane wetting depends on the membrane pore size, the liquid and gas pressure difference (known as the transmembrane pressure, $\Delta P_{L\text{-}G}$), the type of liquid absorbent, and the interactions between the absorbent and the membrane. The wetting ratio, ʒ represents the proportion of the membrane pore that is filled with the liquid, as shown in Figure 1(b) and defined as:

$$ʒ = \frac{r_2 - r_w}{r_2 - r_1} \tag{2}$$

where r_w, r_1 and r_2 are the wetted, inner and outer radii, respectively.

According to Laplace-Young equation, a pore is wetted when the transmembrane pressure ΔP_{L-G} is higher than the breakthrough pressure, ΔP_c given by:

$$\Delta P_c = \frac{-2\,\gamma\cos\theta}{\delta} \tag{3}$$

where γ denotes the surface tension of the liquid phase; θ, the contact angle of the liquid on the membrane; and δ, the pore radius.

In partially-wetted operation, larger pores are filled first, followed by smaller ones. In order to prevent membrane wetting and bubble formation, the MBC should be operated in such a way that $\Delta P_c > \Delta P_{L\text{-}G} > 0$. However, pressure drops along the hollow fibre can increase the transmembrane pressure, and thus result in (partial) membrane wetting. In counter-current operation, partial wetting is more likely near the liquid feed section.

The pressures in the gas and liquid phases at the tube and shell sides, respectively, can be modelled using the Hagen-Poiseuille, Kozeny and static head equations. For instance, with a vertical module in counter-current configuration:

$$P_t(z) = P_g^{in} - \frac{32\mu_g v_{z,g}(L-z)}{1000(2r_1)^2} + \frac{\rho_g g(L-z)}{1000} \tag{4}$$

$$P_s(z) = P_l^{out} + \frac{4\mu_l v_{z,l}\emptyset^2(L-z)}{1000\, r_2[(1-\emptyset)]^2} + \frac{\rho_l g(L-z)}{1000} \tag{5}$$

with $\mu_g, \mu_l, \rho_g, \rho_l, \emptyset, g, z$ denoting the dynamic viscosities (kg m^{-1} s^{-1}), densities (kg m^{-3}) of the gas and liquid phases, packing density, gravitational acceleration (m s^{-2}), and axial position (m), respectively.

The transmembrane pressure, as a function of the axial position, is given by:

$$\Delta P_{L-G}(z) = P_s(z) - P_t(z) \tag{6}$$

It is seen from Eq. (3) that a non-uniform pore size distribution will cause different breakthrough pressure ΔP_c in a given module. Such a distribution is often found to follow a log-normal distribution (Lu et al. 2008), given by:

$$f(\delta) = \frac{1}{\sqrt{2\pi \ln(1+\sigma^2)}\delta} \exp\left(-\frac{\left(\ln\frac{\delta}{\delta^*}\right)^2 (1+\sigma^2)}{2\ln(1+\sigma^2)}\right) \quad (7)$$

where σ and δ^* stand for the standard deviation and mean pore radius, respectively. This way, the wetting ratio ʒ is computed as (Wang et al. 2013):

$$ʒ = \frac{\int_{\delta_w}^{\delta_{\max}} f(\delta)d\delta}{\int_0^{\delta_{\max}} f(\delta)d\delta} \quad \text{with} \quad \delta_w := \frac{-2\gamma\cos\theta}{\Delta P_{L-G}} \quad (8)$$

and r_w can be determined from Eq. (2) in turn.

3 Numerical Case Study

We consider industrially relevant operating conditions for an application in natural gas sweetening with MDEA as the solvent, as given in Hoff & Svendsen (2013), and listed in Table 2 below.

Table 2: *Simulation conditions.*

Parameters	Values
CO_2 inlet, $C_{CO_2}^{in}$ (mol%)	10
MDEA solvent inlet, C_{Sol}^{in} (M)	1
Inlet gas pressure, P_g^{in} (kPa)	7000
Outlet liquid pressure, P_l^{out} (kPa)	7020
Gas flow (actual,m^3 h^{-1})	8 381
Liquid flow (actual,m^3 h^{-1})	1 429
Gas temperature (K)	313
Liquid temperature (K)	313

The diffusivities of a species *i* in the gas and liquid phases are estimated from empirical correlations based on kinetic gas theory (Faiz & Al-Marzouqi 2010) and the analogy of N_2O diffusivity in solution (Wang et al. 2013), respectively. The diffusivity coefficients in the membrane consider the effect of porosity and tortuosity as given by (Faiz & Al-Marzouqi 2010) :

$$D_{CO_2,md} = \frac{\varepsilon}{\tau} D_{CO_2,g} \quad (9)$$

$$D_{i,mw} = \frac{\varepsilon}{\tau} D_{i,l} \quad (10)$$

At r_w, the relationship of Henry's constant, *H* and the dimensionless distribution coefficient, *m* is given by:

$$m = \frac{1000RT}{H} \quad (11)$$

where *T* is the temperature of the liquid phase (K) and *R* = 8.314 m^3 Pa mol^{-1} K^{-1} is the ideal gas constant. Henry's constant for CO_2 in amine solution can also be calculated by the N_2O analogy. The reaction rate and reaction rate constant MDEA is given by (Lu et al. 2007):

$$R_i = -k_{\text{MDEA}}\, C_{CO_2}\, C_{MDEA} \quad (12)$$

$$k_{\text{MDEA}} = 4.01 \times 10^5 \exp\left(-\frac{5400}{T}\right) \quad (13)$$

Finally, the hollow-fibre membranes and the module specifications are taken from Lu et al. (2008) and Hoff & Svendsen (2013), respectively, as listed in Table 3.

Table 3**:** *Specifications of the hollow-fibre membranes and modules.*

	Module I	Module II
Inner radius, r_1 (μm)	150	150
Outer radius, r_2 (μm)	200	250
Porosity, ε (-)	0.45	0.60
Tortuosity, τ (-)	3.3	5.3
Contact angle, θ (°)	93	93
Average pore size, δ^* (μm)	0.015	0.025
Maximum pore size, $\delta_{\max}$ (μm)	0.12	0.29
Standard deviation, σ	0.198	0.268
Membrane Thickness (μm)	50	100
Specific surface area (m^2 m^{-3})	4318	3454
Module diameter (m)	2.4	
Length of fibre, *L* (m)	4.5	
Packing density, ∅ (%)	50	

The model equations associated with the tube, membrane and shell with appropriate boundary conditions and properties from Tables 1-3 are solved using gPROMS Modelbuilder v4.1, which implements a centered finite difference method to discretize the partial differential equations (PDEs). In addition, gPROMS offers an interface with a physical property package to calculate the thermo-physical properties of the chemical phases, such as density, viscosity, surface tension, etc.

4 Results and Discussions

4.1 Effect of Membrane Specifications

Figure 3(i) shows how the transmembrane pressure and the wetting ratio vary along the fibre length in Module I and II. The highest transmembrane pressure is obtained at the position of z = 0, corresponding to the liquid inlet. It can be seen that Module I, whose membranes have smaller pores, is predicted to be non-wetted, whereas those in Module II are partially wetted, even though the transmembrane pressures are comparable since the module diameters are identical. Also note that a transmembrane pressure of at least 20 kPa is maintained at any point along the fibres in order to prevent bubble formation. Figure 3(ii) shows the effect on the CO_2 removal efficiency of the average wetting

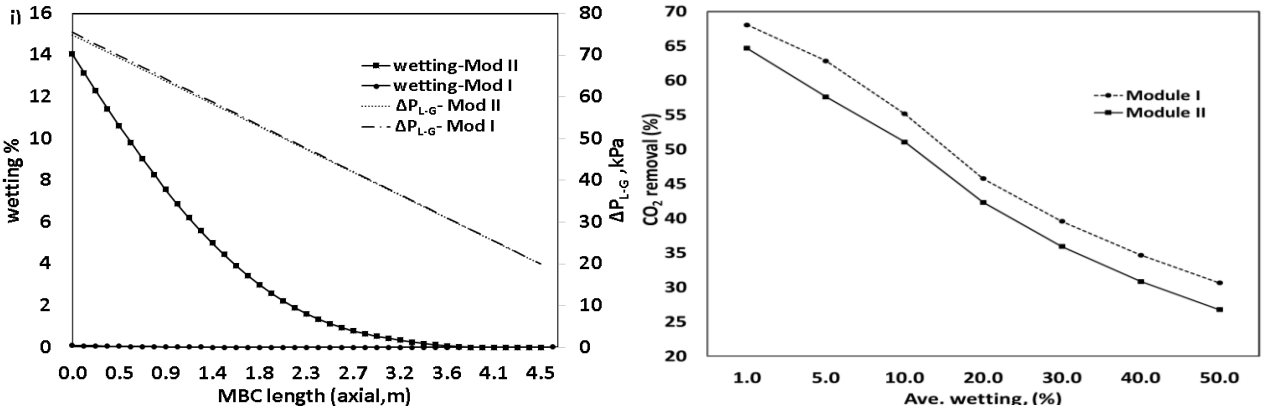

***Figure 3**: (i) Relationship between the transmembrane pressure and the wetting ratio along the fibre length in Modules I and II; (ii) Effect of the average wetting ratio on the CO_2 removal efficiency in Module I and II*

ratio in both modules under the same operating conditions. As expected, a higher wetting increases the mass-transfer resistance thereby leading to a reduction in the CO_2 removal efficiency. This comparison also shows that the effect in terms of CO_2 removal efficiency of a larger porosity may be negated by a thicker membrane with bigger pore sizes and higher membrane tortuosity.

4.2 Effect of Liquid Flow rate

Figure 4 depicts the effect of the liquid velocity on the membrane wetting and the CO_2 absorption flux. It is found that about doubling the liquid flow rate results in a 20% increase in the wetting ratio. This increased wetting is due to a higher pressure drop in the liquid at the shell side, and therefore a higher transmembrane pressure, in agreement with Eq. (5). It is also found that increasing the liquid flow rate improves the CO_2 absorption flux in spite of the extra membrane wetting. This behaviour may be explained by a larger concentration gradient of CO_2 in the solvent, which leads to a better mass transfer as the liquid flow rate increases. These results also suggest that the MBC performance is, to a large extent, dominated by the physic-chemical processes taking place in the liquid phase, a behaviour that has already been reported elsewhere (Boributh et al. 2011).

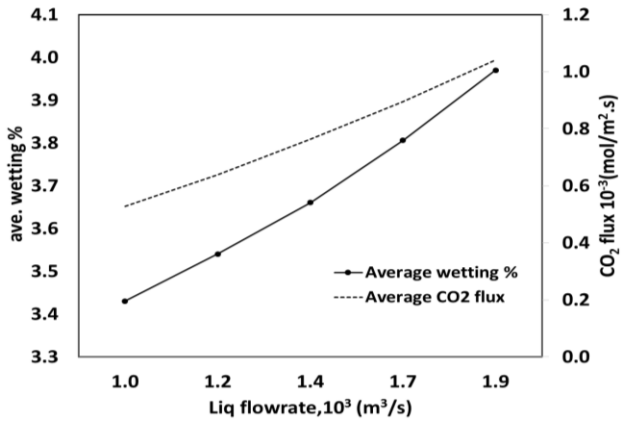

***Figure 4:** Effect of the liquid flow rate on membrane wetting and CO_2 absorption in Module II*

4.3 Effect of MBC Operating Temperature

Figure 5 illustrates the effect of a module's operating temperature on both the membrane wetting and CO_2 absorption flux. On the one hand, the reaction rate and the diffusivity of CO_2 and MDEA increase with the gas and liquid temperatures, leading to a better mass transfer. On the other hand, the gas concentration and the distribution coefficient decrease due to the effect of higher temperature on Henry's constant for the latter, while the gas velocity increases, which limits mass transfer. In addition, a temperature rise reduces the liquid surface tension and the fluid densities and viscosities, which also have a direct effect on the transmembrane pressure $\Delta P_{L\text{-}G}$ and the wetting ratio ʒ. The MBC model can be used to investigate the net effect of varying the operating temperature on CO_2 removal. Nearly no effect of the temperature on the wetting ratio is predicted, which may be explained by the decrease in surface tension being compensated for by the decrease of $\Delta P_{L\text{-}G}$ due to a decrease in fluid densities and viscosities. In contrast, a 20 K temperature rise results in a 10% increase in the CO_2 absorption flux, thereby indicating that the effects of a faster reaction and better diffusivities of CO_2 and MDEA dominates over the reduction in distribution coefficient and mass transfer time in Module II.

4.4 Effect of Module Orientation

We start by noting that operating lab-scale modules vertically or horizontally, under the same operating conditions, does not show significant differences in terms of CO_2 removal performance. However, the impact of operating at a larger-scale MBC under different orientations for natural gas sweetening applications needs closer investigation.

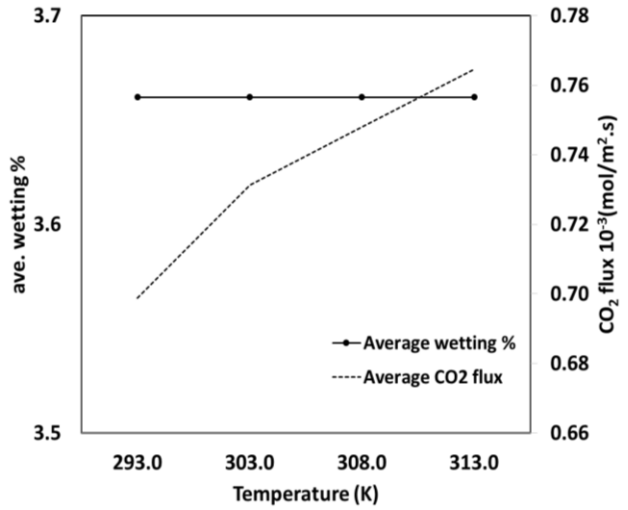

***Figure 5**: Effect of the module operating temperature on membrane wetting and CO_2 absorption in Module II.*

Figure 6 depicts the effect of operating the MBC vertically and horizontally on the membrane wetting. It is seen that operating the MBC horizontally would reduce the transmembrane pressure along the fibres compared with a vertical mode of operation, due to a reduced static head. In turn, this reduced membrane wetting would enhance the CO_2 absorption flux in the horizontal mode of operation.

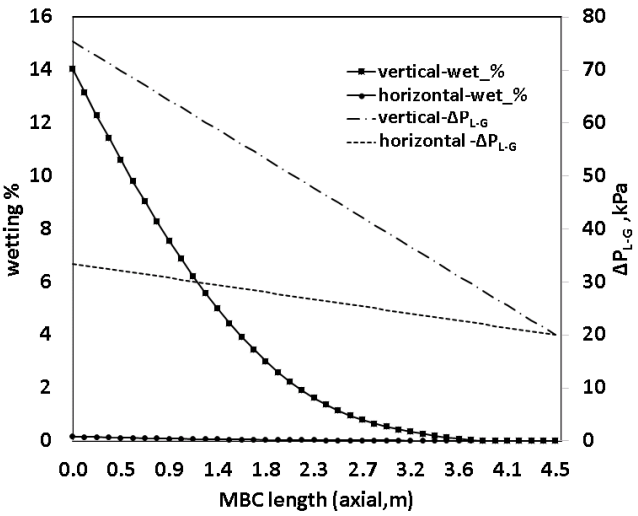

***Figure 6**: Comparison of the wetting ratio and transmembrane pressure in Module II under horizontal and vertical orientations.*

5 Conclusions

A mathematical model of MBC using chemical solvent has been developed, which accounts for the membrane pore size distribution for improved prediction of the membrane wetting and CO_2 removal in commercial natural gas sweetening applications. This model has been used to analyse the effect of the membrane characteristics, key operating conditions, and different module operations. In the studied MBC configurations, a larger liquid flow rate has been shown to increase the CO_2 absorption flux, even though it may also lead to an increase in membrane wetting. Increasing the MBC operating temperature by up to 20 K has also been shown to be beneficial in terms of the CO_2 removal efficiency. Finally, it is shown that operating a large-scale MBC horizontally may reduce the membrane wetting and improve the CO_2 removal efficiency compared to a vertical mode of operation, due to a reduced static head.

Acknowledgments

The authors gratefully acknowledge financial support from PETRONAS.

References

Boributh, S. et al., 2011. A modeling study on the effects of membrane characteristics and operating parameters on physical absorption of CO_2 by hollow fibre membrane contactor. *Journal of Membrane Science*, vol. 380(1-2), pp. 21–33.

Chabanon, E., Roizard, D. & Favre, E., 2013. Modeling strategies of membrane contactors for post-combustion carbon capture: a critical comparative study. *Chemical Engineering Science*, vol. 87, pp. 393–407.

Cui, L. et al., 2015. Modelling and experimental study of membrane wetting in microporous hollow fibre membrane contactors. *The Canadian Journal of Chemical Engineering*, vol. 93(7), pp. 1254–1265.

Faiz, R. & Al-Marzouqi, M., 2010. CO_2 removal from natural gas at high pressure using membrane contactors: model validation and membrane parametric studies. *Journal of Membrane Science*, vol. 365(1-2), pp. 232–241.

Hoff, K.A. & Svendsen, H.F., 2013. CO2 absorption with membrane contactors vs. packed absorbers - challenges and opportunities in post combustion capture and natural gas sweetening. *Energy Procedia*, vol. 37(1876), pp. 952–960.

Lu, J.G. et al., 2007. Effects of activators on mass-transfer enhancement in a hollow fibre contactor using activated alkanolamine solutions. *Journal of Membrane Science*, 289(1-2), pp.138–149.

Lu, J.G., Zheng, Y.F. & Cheng, M.D., 2008. Wetting mechanism in mass transfer process of hydrophobic membrane gas absorption. *Journal of Membrane Science*, vol. 308(1-2), pp. 180–190.

Mansourizadeh, A. & Ismail, A.F., 2009. Hollow fibre gas-liquid membrane contactors for acid gas capture: a review. *Journal of Hazardous Materials*, vol. 171, pp.38–53.

Wang, R. et al., 2005. Influence of membrane wetting on CO_2 capture in microporous hollow fibre membrane contactors. *Separation & Purification Technology*, vol. 46(1-2), pp. 33–40.

Wang, Z. et al., 2013. Experimental and modeling study of trace CO_2 removal in a hollow-fibre membrane contactor, using CO_2-loaded monoethanolamine. *Industrial & Engineering Chemistry Research*, vol. 52, pp. 18059–18070.